

Open Access Full Text Article



Research Article

ADMET-informatics, Pharmacokinetics, Drug-likeness and Medicinal Chemistry of Bioactive Compounds of *Physalis minima* Ethanolic Leaf Extract (PMELE) as a Potential Source of Natural Lead Molecules for Next Generation Drug Design, Development and Therapies

Ramya S.¹, Sutha S.², Chandran M.³, Priyanka R.³, Loganathan T.⁴, Pandiarajan G.⁵, Kaliraj P.⁶, Grace Lydial Pushpalatha G⁷, Abraham GC.⁸ Jayakumararaj R.^{9*}

¹ PG Department of Zoology, Yadava College (Men), Thiruppallai - 625014, Madurai, TN, India

² Department of Medicinal Botany, Govt. Siddha Medical College, Palayamkottai, Tamil Nadu, India

³ Department of Zoology, Thiruvalluvar University, Serkodu, Vellore-632115, India

⁴ Department of Plant Biology & Plant Biotechnology, LN Government College (A), Ponneri, TN, India

⁵ Department of Botany, Sri S Ramasamy Naidu Memorial College (A), Sattur - 626203, TN, India

⁶ Department of Zoology, Sri S Ramasamy Naidu Memorial College (A), Sattur - 626203, TN, India

⁷ PG Department of Botany, Sri Meenakshi Government Arts College, Madurai - 625002, TN, India

⁸ PG & Research Department of Botany, The American College, Madurai - 625002, TamilNadu, India

⁹ Department of Botany, Government Arts College, Melur - 625106, Madurai District, TN, India

Article Info:



Article History:

Received 02 Sep 2022

Reviewed 06 Oct 2022

Accepted 11 Oct 2022

Published 15 Oct 2022

Cite this article as:

Ramya S, Sutha S, Chandran M, Priyanka R, Loganathan T, Pandiarajan G, Kaliraj P, Grace Lydial Pushpalatha G, Abraham GC, Jayakumararaj R, ADMET-informatics, Pharmacokinetics, Drug-likeness and Medicinal Chemistry of Bioactive Compounds of *Physalis minima* Ethanolic Leaf Extract (PMELE) as a Potential Source of Natural Lead Molecules for Next Generation Drug Design, Development and Therapies, Journal of Drug Delivery and Therapeutics. 2022; 12(5):188-200

DOI: <http://dx.doi.org/10.22270/jddt.v12i5.5654>

*Address for Correspondence:

Dr. R. Jayakumararaj, Department of Botany, Government Arts College, Melur - 625106, Madurai District, TN, India

Abstract

Physalis minima (PM) belongs to the family Solanaceae. PM has been traditionally used to cure and prevent several disorders as documented in Vedic Texts. Nevertheless, scientific values of traditional claims haven't been explored yet. In the previous study, GCMS analysis of *P. minima* ethanolic leaf extracts (PMELE) indicated the presence of Cyclobutanol (C₄H₈O); D-Alanine (C₃H₇O₂N); 2-Heptanol, 6-Amino-2-Methyl (C₈H₁₉ON); 1-Pentanol, 4-Amino (C₅H₁₃NO); Benzeneethanamine, 3-Fluoro-Beta,5-Dihydroxy-N-Methyl (C₉H₁₂FN₂O₂) and L-Alanine, N-(N-Acetylglycyl)-, Butyl Ester (C₁₁H₂₀N₂O₄). However, biological activities of these bioactive compounds are not known which hampers the exploitation of these compounds by pharma-industries on a commercial scale. This study on ADMET, Pharmacokinetics, Drug-likeness and Medicinal Chemistry of Bioactive Compounds in PMELE aims to provide baseline information on PBNPs as a potential source of natural lead molecules for next generation drug design, development and therapeutics.

Keywords: PM-PBNPs; ADMET; PMELE; Pharmacokinetics; Drug-likeness; Drug Development; Bioactive Compounds

INTRODUCTION

Secondary metabolite in plants collectively known as Plant Based Natural Products (PBNPs) plays a vital role in human existence and they are considered as foundation of Traditional Indigenous Systems of Medicine (TISM)^{1,2}. Unlike the synthetic drugs that are used for the treatment of various infectious diseases, PBNPs are effective, safe, affordable and are of GRAS standard with fewer side effects³. Meanwhile, WHO has also recognized the importance of TISM and has laid strategies, guidelines and standards for the use of Plant-Based Medicine⁴. This boils down to the fact that medicinal plants are base-resources of new drugs and many of the modern medicines are produced based on the natural chemistry of PBNPs. In recent times, there have been increased interests in research on PBNPs. This is attributed to unmet therapeutic needs,

remarkable diversity structure and functionality of PBNPs, advancement in the field of computing technologies - AI and ML to hunt for PBNPs⁵, therefore, Pharmaceutical Giants are adopting data mining and AI&ML technologies to reduce time and cost required for R&D program⁶⁻¹².

Alternatively, development of novel and sensitive techniques to detect biologically active PBNPs, advanced techniques to isolate, purify and structurally characterize PBNPs, and advances to meet out demand-supply aspects of PBNPs have prompted interest in development and promotion of herbal drugs. In recent years, both combinatorial chemistry and high-throughput screening platforms have significantly increased the number of compounds for which early data on absorption, distribution, metabolism, excretion (ADME) and toxicity (T) are not available, which has led to the development of a

variety of medium and high-throughput in vitro ADMET screens for drug development and design with deeper dimension with high degree of precision taking into account cost economics and time⁵⁻¹⁹.

Immense medicinal properties of bioactive compounds from *Physalis* have generated interest in extracting and characterizing compounds that its different species possess and identifying the active withanolides responsible for their unique medicinal properties²⁰⁻²³. It has been pointed out that withanolides are intriguing principal compounds for inflammatory, neuro-inflammatory and cancer treatment due to unique steroid structure and specific bioactivities²³.

MATERIALS AND METHODS

In silico Drug-Likeliness and Bioactivity Prediction

The drug likeliness and bioactivity of selected molecule was analyzed using the Molinspiration server (<http://www.molinspiration.com>). Molinspiration tool is cheminformatics software that provides molecular properties as well as bioactivity prediction of compounds²⁴. In Molinspiration-based drug-likeness analysis, there are two important factors, including the lipophilicity level (log P) and polar surface area (PSA) directly associated with the pharmacokinetic properties (PK) of the compounds²⁵. In Molinspiration-based bioactivity analysis, the calculation of the bioactivity score of compounds toward GPCR ligands, ion channel modulators, kinase inhibitors, nuclear receptor ligands, protease inhibitors, and other enzyme targets were analyzed by Bayesian statistics^{26,27}. This was carried out for G protein-coupled receptors (GPCR), ion channels, kinases, nuclear hormone receptors, proteases, and other enzymes (RdRp), are the major drug targets of most of the drugs²⁸.

In silico ADMET Analysis

SwissADME: is a Web tool that gives free access to a pool of fast yet robust predictive models for physicochemical properties, pharmacokinetics, druglikeness and medicinal chemistry friendliness, among which in-house proficient methods such as iLOGP (a physics-based model for lipophilicity) or the BOILED-Egg (an intuitive graphical classification model for gastrointestinal absorption and brain access). It is the first online tool that enables ADME-related calculation for multiple molecules, allowing chemical library analysis and efficient lead optimization²⁹. PK properties, such as Absorption, Distribution, Metabolism, Excretion, and Toxicity (ADMET), of fatty acids were predicted using admerSAR v2.0 server (<http://lmmd.ecust.edu.cn/admetsar2/>) and The admerSAR server is an open-source computational tool for prediction of ADMET properties of compounds, which makes it a practical platform for drug discovery and other pharmacological research³⁰.

In ADMET analysis, absorption (A) of good drugs depends on factors such as membrane permeability³¹ [designated by colon cancer cell line (Caco-2)], human intestinal absorption (HIA)³², and status of either P-glycoprotein substrate or inhibitor³³. Distribution (D) of drugs mainly depends on the ability to cross blood-brain barrier (BBB)³⁴. The metabolism (M) of drugs is calculated by the CYP, MATE1, and OATP1B1-OATP1B3 models³⁵. Excretion (E) of drugs is estimated based on the renal OCT substrate. Toxicity (T) of drugs is predicted on Human Ether-A-Go-Go related gene inhibition, carcinogenic status, mutagenic status, and acute oral toxicity³⁶.

vNN model building and analysis

vNN method was used to calculate the similarity distance between molecules in terms of their structure, and uses a distance threshold to define a domain of applicability to

ensures that the predictions generated are reliable. vNN models can be built keeping quantitative structure-activity relationship (QSAR) models up-to-date to maintain their performance levels. Performance characteristics of the models are comparable, and often superior to those of other more elaborate model.³⁸⁻⁴⁹ One of the most widely used measures of similarity distance between two small molecules is Tanimoto distance, d, which is defined as:

$$d = 1 - \frac{n(P \cap Q)}{n(P) + n(Q) - (P \cap Q)}$$

where $n(P \cap Q)$ is number of features common to molecules p and q, and $n(P)$ and $n(Q)$ are the total numbers of features for molecules p and q, respectively. The predicted biological activity y is given by a weighted across structurally similar neighbours:

$$y = \frac{\sum_{i=1}^v y_i e^{-(di/h)^2}}{\sum_{i=1}^v e^{-(di/h)^2}} \quad di \leq d_0$$

where di denotes Tanimoto distance between a query molecule for which a prediction is made and a molecule i of the training set; d_0 is a Tanimoto-distance threshold, beyond which two molecules are no longer considered to be sufficiently similar to be included in the average; y_i is the experimentally measured activity of molecule i ; v denotes the total number of molecules in the training set that satisfies the condition $di \leq d_0$; and h is a smoothing factor, which dampens the distance penalty. Values of h and d_0 are determined from cross-validation studies. To identify structurally similar compounds, Accelrys Extended-Connectivity FingerPrints with a diameter of four chemical bonds (ECFP4) were used³⁸⁻⁴⁰.

Model Validation

A 10-fold cross-validation (CV) procedure was used to validate new models and to determine the values of smoothing factor h and Tanimoto distance d_0 . In this procedure, data was randomly divided into 10 sets, and used 9 to develop the model and 10th to validate it, this process was repeated 10 times, leaving each set of molecules out once.

Performance Measures

Following metrics were used to assess model performance. (1) sensitivity measures a model's ability to correctly detect true positives, (2) specificity measures a model's ability to detect true negatives, (3) accuracy measures a model's ability to make correct predictions and (4) kappa compares the probability of correct predictions to the probability of correct predictions by chance (its value ranges from +1 (perfect agreement between model prediction and experiment) to -1 (complete disagreement), with 0 indicating no agreement beyond that expected by chance).

$$\text{sensitivity} = \frac{\text{TP}}{\text{TP} + \text{FN}}$$

$$\text{specificity} = \frac{\text{TN}}{\text{FP} + \text{TN}}$$

$$\text{accuracy} = \frac{\text{TP} + \text{TN}}{\text{TP} + \text{TN} + \text{FP} + \text{FN}}$$

$$\kappa = \frac{\text{accuracy} - \text{Pr}(e)}{1 - \text{Pr}(e)}$$

where TP, TN, FP, and FN denote the numbers of true positives, true negatives, false positives, and false negatives, respectively. Kappa is a metric for assessing the quality of binary classifiers. Pr (e) is an estimate of the probability of a correct prediction by chance. It is calculated as:

$$\text{Pr}(e) = \frac{(TP + FN)(TP + FP) + (TP + FN)(TP + FP)}{(TP + FN + FP + TN)^2}$$

The coverage is the proportion of test molecules with at least one nearest neighbour that meets the similarity criterion. The coverage is a measure of how many test compounds are within the applicability domain of a prediction model³⁷⁻⁴⁰. OSIRIS Property Explorer an integral part of Actelion's in-house substance registration system was used to calculate on-the-fly various drug-relevant properties for drawn chemical structures, including some toxicity and druglikeness properties.

RESULTS AND DISCUSSION

GCMS analysis ethanolic leaf extracts of *P. minima* indicated the presence of (at RT in min) 2.528 - Cyclobutanol (C₄H₈O); 2.598 - D-Alanine (C₃H₇O₂N); 6.145 - 2-Heptanol, 6-Amino-2-Methyl (C₈H₁₉ON); 7.821 - 1-Pentanol, 4-Amino (C₅H₁₃NO); 8.401 - Benzeneethanamine, 3-Fluoro-Beta,,5-Dihydroxy-N-Methyl (C₉H₁₂FNO₂); 29.339 - L-Alanine, N-(N-Acetylglycyl)-, Butyl Ester (C₁₁H₂₀N₂O₄) were detected in the ethanolic leaf extracts of *P. minima* respectively (Table 1a, b; Fig. 1).

Drug-likeness properties of PM-PBNPs

The drug score value combines all other predictions into one grand total. Based on this logic the Score from cLogP: 0.581 (cLogP = 4.672); Score from logS: 0.847 (logS = -3.286); Score from molecular weight: 0.968 (molecular weight 214.0); Score from drug-likeness: 0.0 (drug-likeness = 35.364); No Risk of Mutagenicity Score = 1.0; No Risk of Irritating Effects Score = 1.0; No Risk of Reproductive Effects Score = 1.0 respectively were predicted and the overall predicted drug score for compound 1 was calculated as 0.359. Score from cLogP: 0.680 (cLogP = 4.244); Score from logS: 0.863 (logS = -3.158); Score from molecular weight: 0.973 (molecular weight 200.0); Score from drug-likeness: 0.0 (drug-likeness = 25.215); No Risk of Mutagenicity Score = 0.6; No Risk of Irritating Effects Score = 0.6; No Risk of Reproductive Effects Score = 1.0 respectively were predicted and the overall predicted drug score for compound 2 was calculated as 0.083.

Score from cLogP: 0.358 (cLogP = 5.581); Score from logS: 0.763 (logS = -3.826); Score from molecular weight: 0.956 (molecular weight 242.0); Score from drug-likeness: 0.0 (drug-likeness = 35.364); No Risk of Mutagenicity Score = 1.0; No Risk of Irritating Effects Score = 1.0; No Risk of Reproductive Effects Score = 1.0 respectively were predicted and the overall predicted drug score for compound 3 was calculated as 0.293. Score from cLogP: 0.183 (cLogP = 6.49); Score from logS: 0.653 (logS = -4.366); Score from molecular weight: 0.94 (molecular weight 270.0); Score from drug-likeness: 0.0 (drug-likeness = 35.364); No Risk of Mutagenicity Score = 1.0; No Risk of Irritating Effects Score = 1.0; No Risk of Reproductive Effects Score = 1.0 respectively were predicted and the overall predicted drug score for compound 4 was calculated as 0.237.

Score from cLogP: 0.256 (cLogP = 6.062); Score from logS: 0.681 (logS = -4.239); Score from molecular weight: 0.949

(molecular weight 256.0); Score from drug-likeness: 0.0 (drug-likeness = 25.215); No Risk of Mutagenicity Score = 1.0; No Risk of Tumorigenicity Score = 0.6; No Risk of Irritating Effects Score = 0.6; No Risk of Reproductive Effects Score = 1.0 respectively were predicted and the overall predicted drug score for compound 5 was calculated as 0.092. Score from cLogP: 0.104 (cLogP = 7.147); Score from logS: 0.579 (logS = -4.678); Score from molecular weight: 0.920 (molecular weight 296.0); Score from drug-likeness: 0.0 (drug-likeness = -30.917); No Risk of Mutagenicity Score = 1.0; No Risk of Tumorigenicity Score = 1.0; No Risk of Irritating Effects Score = 1.0; No Risk of Reproductive Effects Score = 1.0 respectively were predicted and the overall predicted drug score for compound 6 was calculated as 0.209.

Score from cLogP: 0.083 (cLogP = 7.399); Score from logS: 0.523 (logS = -4.906); Score from molecular weight: 0.918 (molecular weight 298.0); Score from drug-likeness: 0.0 (drug-likeness = 35.364); No Risk of Mutagenicity Score = 1.0; No Risk of Tumorigenicity Score = 1.0; No Risk of Irritating Effects Score = 1.0; No Risk of Reproductive Effects Score = 1.0 respectively were predicted and the overall predicted drug score for compound 7 was calculated as 0.197. Score from cLogP: 0.384 (cLogP = 5.469); Score from logS: 0.647 (logS = -4.428); Score from molecular weight: 0.882 (molecular weight = 332.0); Score from drug-likeness: 0.0 (drug-likeness = -7525); No Risk of Mutagenicity Score = 1.0; No Risk of Tumorigenicity Score = 1.0; No Risk of Irritating Effects Score = 1.0; No Risk of Reproductive Effects Score = 1.0 respectively were predicted and the overall predicted drug score for compound 8 was calculated as 0.267.

Bio-molecular properties of PM-PBNPs

Calculated value for molecular properties of compound 1 were (values given in parenthesis) - miLogP (5.35); TPSA (26.30); Natoms (15); MW (214.35); nON (2); nOHNH (0); Nviolations (1); Nrotb (11); volume (214.74) respectively; and the calculated bioactivity scores for biological properties were - GPCR ligand (-0.41); Ion channel modulator (-0.13); Kinase inhibitor (-0.73); Nuclear receptor ligand (-0.43); Protease inhibitor (-0.46); Enzyme inhibitor (-0.11) respectively (**Table 2a**). Calculated value for molecular properties of the compound 2 were - miLogP (5.04); TPSA (37.30); Natoms (14); MW (200.32); nON (2); nOHNH (1); Nviolations (1); Nrotb (10); volume (224.22) respectively; and the calculated bioactivity scores for biological properties were - GPCR ligand (-0.27); Ion channel modulator (-0.04); Kinase inhibitor (-0.75); Nuclear receptor ligand (-0.24); Protease inhibitor (-0.36); Enzyme inhibitor (0.04) respectively (**Table 2b**).

Calculated value for molecular properties of the compound 3 were - miLogP (6.36); TPSA (26.30); Natoms (17); MW (242.40); nON (2); nOHNH (0); Nviolations (1); Nrotb (13); volume (275.35) respectively; and the calculated bioactivity scores for biological properties were - GPCR ligand (-0.24); Ion channel modulator (-0.07); Kinase inhibitor (-0.51); Nuclear receptor ligand (-0.24); Protease inhibitor (-0.28); Enzyme inhibitor (-0.02) respectively (**Table 2c**). Calculated value for molecular properties of the compound 4 were - miLogP (7.37); TPSA (26.30); Natoms (19); MW (270.46); nON (2); nOHNH (0); Nviolations (1); Nrotb (15); volume (308.95) respectively; and the calculated bioactivity scores for biological properties were - GPCR ligand (-0.11); Ion channel modulator (-0.05); Kinase inhibitor (-0.34); Nuclear receptor ligand (-0.09); Protease inhibitor (-0.13); Enzyme inhibitor (-0.04) respectively (**Table 2d**).

Calculated value for molecular properties of the compound 5 were - miLogP (7.06); TPSA (37.30); Natoms (18); MW (256.43); nON (2); nOHNH (1); Nviolations (1); Nrotb (14); volume (291.42) respectively; and the calculated bioactivity

scores for biological properties were - GPCR ligand (0.02); Ion channel modulator (0.06); Kinase inhibitor (-0.33); Nuclear receptor ligand (0.08); Protease inhibitor (-0.04); Enzyme inhibitor (0.18) respectively (**Table 2e**). Calculated value for molecular properties of the compound 6 were - miLogP (7.89); TPSA (26.30); Natoms (21); MW (296.50); nON (2); nOHNH (0); Nviolations (1); Nrotb (16); volume (336.37) respectively; and the calculated bioactivity scores for biological properties were - GPCR ligand (0.03); Ion channel modulator (-0.03); Kinase inhibitor (-0.25); Nuclear receptor ligand (0.06); Protease inhibitor (-0.02); Enzyme inhibitor (0.12) respectively (**Table 2f**).

Calculated value for molecular properties of the compound 7 were - miLogP (8.32); TPSA (26.30); Natoms (21); MW (298.51); nON (2); nOHNH (0); Nviolations (1); Nrotb (17); volume (342.55) respectively; and the calculated bioactivity scores for biological properties were - GPCR ligand (-0.03); Ion channel modulator (-0.04); Kinase inhibitor (-0.23); Nuclear receptor ligand (0.00); Protease inhibitor (-0.03); Enzyme inhibitor (0.05) respectively (**Table 2g**). Calculated value for molecular properties of the compound 8 were - miLogP (4.32); TPSA (17.07); Natoms (24); MW (332.47); nON (1); nOHNH (0); Nviolations (0); Nrotb (5); volume (308.98) respectively; and the calculated bioactivity scores for biological properties were - GPCR ligand (0.15); Ion channel modulator (0.08); Kinase inhibitor (0.10); Nuclear receptor ligand (0.01); Protease inhibitor (0.27); Enzyme inhibitor (0.20) respectively (**Table 2h**). The pink area (Fig. 2) represents the optimal range for each property (lipophilicity: XLOGP3 between -0.7 and +5.0, size: MW between 150 and 500 g/mol, polarity: TPSA between 20 and 130 Å², solubility: log S not higher than 6, saturation: fraction of carbons in the sp³ hybridization not less than 0.25, and flexibility: no more than 9 rotatable bonds). The overall Natural Product Likeness Score for PBNPs from *P. minima* is shown in Fig. 3

ADMET and Pharmacokinetic properties of PM-PBNPs

Absorption, Distribution, Metabolism, Excretion and Toxicity (ADMET) prediction models, including their performance measures as discussed in previous studies. 15 models cover a diverse set of ADMET endpoints. Some of the models have already been published, including those for Maximum Recommended Therapeutic Dose (MRTD), chemical mutagenicity, human liver microsomal (HLM), Pgp inhibitor/substrates.⁴²

Liver Toxicity

DILI: Drug-induced liver injury (DILI) has been one of the most commonly cited reason for drug withdrawals from the market. This application predicts whether a compound could cause DILI. The dataset of 1,431 compounds was obtained from four sources used by Xu et al.⁴⁸ This dataset contains both pharmaceuticals and non-pharmaceuticals; classified as compound as causing DILI if it was associated with a high risk of DILI and not if there was no such risk Table 3.

Cytotoxicity (HepG2): Cytotoxicity is the degree to which a chemical causes damage to cells. Cytotoxicity prediction model was developed, using in vitro data on toxicity against HepG2⁵⁰ cells for 6,000 structurally diverse compounds, collected from ChEMBL for compounds with an IC₅₀ ≤ 10 μM in the in vitro assay as cytotoxic Table 3.

Metabolism

HLM: Human Liver Microsomal (HLM)⁴² stability assay is commonly used to identify and exclude compounds that are too rapidly metabolized. For a drug to achieve effective therapeutic concentrations in the body, it cannot be metabolized too rapidly by the liver. Compounds with a half-

life of 30 min or longer in an HLM assay are considered as stable; otherwise they are considered unstable. HLM data was retrieved from the ChEMBL database, manually curated the data, and classified compounds as stable or unstable based on the reported half-life (T_{1/2} > 30 min was considered stable, and T_{1/2} < 30 min unstable. The final dataset contained 3,654 compounds. Of these, 2,313 compounds were classified as stable and 1,341 compounds were classified as unstable Table 3.⁴²

Cytochrome P450 enzyme (CYP) inhibition: CYPs constitute a superfamily of proteins that play an important role in the metabolism and detoxification of xenobiotics⁵¹. In-vitro data derived from five main drug-metabolizing CYPs—1A2, 3A4, 2D6, 2C9, and 2C19 were used to develop CYP inhibition models. CYP inhibitors were retrieved from PubChem and classified a compound with an IC₅₀ ≤ 10 μM for an enzyme as an inhibitor of the enzyme. Predictions for the following enzymes have been provided CYP1A2, CYP3A4, CYP2D6, CYP2C9, and CYP2C19 Table 3.

Membrane Transporters

BBB: Blood-Brain Barrier (BBB) is a highly selective barrier that separates the circulating blood from the central nervous system. vNN-based BBB model was developed, using 352 compounds whose BBB permeability values (logBB) were obtained from the literature respectively.^{34,47} Classified compounds with logBB values of less than -0.3 and greater than +0.3 as BBB non-permeable and permeable Table 3, (Fig. 4).

Pgp Substrates and Inhibitors: P-glycoprotein (Pgp) is an essential cell membrane protein that extracts many foreign substances from the cell. Cancer cells often overexpress Pgp, which increases the efflux of chemotherapeutic agents from the cell and prevents treatment by reducing effective intracellular concentrations of such agents - a phenomenon known as MDR. For this reason, identifying compounds that can either be transported out of the cell by Pgp (substrates) or impair Pgp function (inhibitors) is of great interest. Models were developed to predict both Pgp substrates and Pgp inhibitors.⁴⁶ The Pgp substrate dataset was collected by Hou and co-workers.⁴³ The dataset consists of measurements of 422 substrates and 400 non-substrates. To generate a large Pgp inhibitor dataset, we combined two datasets,^{44,45} and removed duplicates to form a combined dataset consisting of a training set of 1,319 inhibitors and 937 non-inhibitors Table 3.

hERG (Cardiotoxicity): The human ether-à-go-go-related gene (hERG) codes for a potassium ion channel involved in the normal cardiac repolarization activity of the heart. Drug-induced blockade of hERG function can cause long QT syndrome, which may result in arrhythmia and death. 282 known hERG blockers were retrieved from the literature and classified compounds with an IC₅₀ cut-off value of 10 μM or less as blockers.³⁸ A set of 404 collected compounds with IC₅₀ values greater than 10 μM from ChEMBL and classified them as non-blockers Table 3.

MMP (Mitochondrial Toxicity): Given the fundamental role of mitochondria in cellular energetics and oxidative stress, mitochondrial dysfunction has been implicated in cancer, diabetes, neurodegenerative disorders, and cardiovascular diseases. Largest dataset of chemical-induced changes in mitochondrial membrane potential (MMP) were used based on the assumption that a compound that causes mitochondrial dysfunction is also likely to reduce the MMP⁴⁰. vNN-based MMP prediction model was developed, using 6,261 compounds collected from a previous study that screened a library of 10,000 compounds (~8,300 unique chemicals) at 15 concentrations, each in triplicate, to measure changes in the MMP in HepG2 cells.¹⁰ Based on the data obtained, it is

concluded that 913 compounds decreased the MMP, whereas 5,395 compounds had no effect Table 3.

Mutagenicity (Ames test): Mutagens are chemicals that cause abnormal genetic mutations leading to cancer. A common way to assess a chemical's mutagenicity is the Ames test. A prediction model was developed, using a literature dataset of 6,512 compounds, of which 3,503 were Ames-positive Table 3.

Maximum Recommended Therapeutic Dose (MRTD): Maximum Recommended Therapeutic Dose (MRTD) is an estimated upper daily dose that is safe. A prediction model was built based on a dataset of MRTD values publically disclosed by FDA, mostly of single-day oral doses for an average adult with a body weight of 60 kg, for 1,220 compounds (most of which are small organic drugs). Organometallics, high-molecular weight polymers were excluded (>5,000 Da), nonorganic chemicals, mixtures of chemicals, and very small molecules (<100 Da). An external test set of 160 compounds that were collected were used for validation. The total dataset for our model contained 1,185 compounds. The predicted MRTD value is reported in mg/day unit based upon an average adult weighing 60 kg. Overall performance measures of vNN models for PBNPs from PMELE is shown in Fig. 5 and the summary of ADMET properties of PBNPs (C1-C8) from PMELE is given in Table 4.

CONCLUSION

Exploring the nutritional, phytochemical and pharmacological potential and food usages drives the hunt for bioactive molecules from plant sources.^{52,53} In the present study eight bioactive compounds has been isolated from ethanolic leaf extracts of *P. minima*. The compounds were ADMET predicted for their potential activity, calculated values for molecular properties of all the molecules were within the functional range. Likewise, bioactivity score for all the selected compounds were within the permissible range. Predicted drug score for all the bioactive molecules were within the consumable range. Overall data depict that these compounds may be used as a potential source of natural lead molecules for next generation drug design development and therapies.

REFERENCES

1. Jain C, Khatana S, Vijayvergia R. Bioactivity of secondary metabolites of various plants: a review. *Int. J. Pharm. Sci. Res.* 2019; 10(2):494-504.
2. Hussein RA, El-Anssary AA. Plants secondary metabolites: the key drivers of the pharmacological actions of medicinal plants. *Herb. Med.* 2019 Jan 30; 1(3). <https://doi.org/10.5772/intechopen.76139>
3. Seca AM, Pinto DC. Plant secondary metabolites as anticancer agents: successes in clinical trials and therapeutic application. *International journal of molecular sciences.* 2018 Jan 16; 19(1):263. <https://doi.org/10.3390/ijms19010263>
4. Shrikumar S, Ravi TK. Approaches towards development and promotion of herbal drugs. *Pharmacog Rev.* 2007 Jan 1; 1(1):180-4.
5. Krishnaveni K, Sabitha M, Murugan M, Kandeepan C, Ramya S, Loganathan T, Jayakumararaj R. vNN model cross validation towards Accuracy, Sensitivity, Specificity and kappa performance measures of β -caryophyllene using a restricted-unrestricted applicability domain on Artificial Intelligence & Machine Learning approach based in-silico prediction. *Journal of Drug Delivery and Therapeutics.* 2022 Feb 22; 12(1-S):123-31. <https://doi.org/10.22270/jddtv12i1-S.5222>
6. Ramya S, Soorya C, Pushpalatha GG, Aruna D, Loganathan T, Balamurugan S, Abraham GC, Ponrathy T, Kandeepan C, Jayakumararaj R. Artificial Intelligence and Machine Learning approach based in-silico ADME-Tox and Pharmacokinetic Profile of α -Linolenic acid from Catharanthus roseus (L.) G. Don. *Journal of Drug Delivery and Therapeutics.* 2022 Apr 15; 12(2-S):96-109. <https://doi.org/10.22270/jddtv12i2-S.5274>
7. Ramya S, Loganathan T, Chandran M, Priyanka R, Kavipriya K, Pushpalatha GG, Aruna D, Ramanathan L, Jayakumararaj R, Saluja V. Phytochemical Screening, GCMS, FTIR profile of Bioactive Natural Products in the methanolic extracts of Cuminum cyminum seeds and oil. *Journal of Drug Delivery and Therapeutics.* 2022 Apr 15; 12(2-S):110-8. <https://doi.org/10.22270/jddtv12i2-S.5280>
8. Kandeepan C, Sabitha M, Parvathi K, Senthilkumar N, Ramya S, Boopathi NM, Jayakumararaj R. Phytochemical Screening, GCMS Profile, and In-silico properties of Bioactive Compounds in Methanolic Leaf Extracts of *Moringa oleifera*. *Journal of Drug Delivery and Therapeutics.* 2022 Mar 15; 12(2):87-99. <https://doi.org/10.22270/jddtv12i2-S.5250>
9. Ramya S, Murugan M, Krishnaveni K, Sabitha M, Kandeepan C, Jayakumararaj R. In-silico ADMET profile of Ellagic Acid from *Syzygium cumini*: A Natural Biaryl Polyphenol with Therapeutic Potential to Overcome Diabetic Associated Vascular Complications. *Journal of Drug Delivery and Therapeutics.* 2022 Jan 15; 12(1):91-101. <https://doi.org/10.22270/jddtv12i1.5179>
10. Kalaimathi RV, Jeevalatha A, Basha AN, Kandeepan C, Ramya S, Loganathan T, Jayakumararaj R. In-silico Absorption, Distribution, Metabolism, Elimination and Toxicity profile of Isopulegol from *Rosmarinus officinalis*. *Journal of Drug Delivery and Therapeutics.* 2022 Jan 15; 12(1):102-8. <https://doi.org/10.22270/jddtv12i1.5188>
11. Parvathi K, Kandeepan C, Sabitha M, Senthilkumar N, Ramya S, Boopathi NM, Ramanathan L, Jayakumararaj R. In-silico Absorption, Distribution, Metabolism, Elimination and Toxicity profile of 9, 12, 15-Octadecatrienoic acid (ODA) from *Moringa oleifera*. *Journal of Drug Delivery and Therapeutics.* 2022 Apr 15; 12(2-S):142-50. <https://doi.org/10.22270/jddtv12i2-S.5289>
12. Soorya C, Balamurugan S, Ramya S, Neethirajan K, Kandeepan C, Jayakumararaj R. Physicochemical, ADMET and Druggable properties of Myricitin: A Key Flavonoid in *Syzygium cumini* that regulates metabolic inflammations. *Journal of Drug Delivery and Therapeutics.* 2021 Jul 15; 11(4):66-73. <https://doi.org/10.22270/jddtv11i4.4890>
13. Loganathan T, Barathinivas A, Soorya C, Balamurugan S, Nagajothi TG, Ramya S, Jayakumararaj R. Physicochemical, Druggable, ADMET Pharmacoinformatics and Therapeutic Potentials of Azadirachtin-a-Prenol Lipid (Triterpenoid) from Seed Oil Extracts of *Azadirachta indica* A. Juss. *Journal of Drug Delivery and Therapeutics.* 2021 Sep 15; 11(5):33-46. <https://doi.org/10.22270/jddtv11i5.4981>
14. Sabitha M, Krishnaveni K, Murugan M, Basha AN, Pallan GA, Kandeepan C, Ramya S, Jayakumararaj R. In-silico ADMET predicated Pharmacoinformatics of Quercetin-3-Galactoside, polyphenolic compound from *Azadirachta indica*, a sacred tree from Hill Temple in Alagarkovil Reserve Forest, Eastern Ghats, INDIA. *Journal of Drug Delivery and Therapeutics.* 2021 Oct 15; 11(5-S):77-84. <https://doi.org/10.22270/jddtv11i5-S.5026>
15. Kandeepan C, Kalaimathi RV, Jeevalatha A, Basha AN, Ramya S, Jayakumararaj R. In-silico ADMET Pharmacoinformatics of Geraniol (3, 7-dimethylocta-trans-2, 6-dien-1-ol)-acyclic monoterpene alcohol drug from Leaf Essential Oil of *Cymbopogon martinii* from Sirumalai Hills (Eastern Ghats), INDIA. *Journal of Drug Delivery and Therapeutics.* 2021 Aug 15; 11(4-S):109-18. <https://doi.org/10.22270/jddtv11i4-S.4965>
16. Krishnaveni K, Murugan M, Kalaimathi RV, Basha AN, Pallan GA, Kandeepan C, Senthilkumar N, Mathialagan B, Ramya S, Jayakumararaj R, Loganathan T. ADMET informatics of Plant Derived n-Hexadecanoic Acid (Palmitic Acid) from ethyl acetate fraction of *Moringa oleifera* leaf extract. *Journal of Drug Delivery and Therapeutics.* 2022 Sep 15; 12(5):132-45. <https://doi.org/10.22270/jddtv12i5.5605>
17. Jeevalatha A, Kalaimathi RV, Basha AN, Kandeepan C, Ramya S, Loganathan T, Jayakumararaj R. Profile of bioactive compounds in *Rosmarinus officinalis*. *Journal of Drug Delivery and Therapeutics.* 2022 Jan 15; 12(1):114-22. <https://doi.org/10.22270/jddtv12i1.5189>
18. Kalaimathi RV, Krishnaveni K, Murugan M, Basha AN, Gilles AP, Kandeepan C, Senthilkumar N, Mathialagan B, Ramya S, Ramanathan L, Jayakumararaj R. ADMET informatics of Tetradecanoic acid (Myristic Acid) from ethyl acetate fraction of *Moringa oleifera* leaves. *Journal of Drug Delivery and Therapeutics.* 2022 Aug 20; 12(4-S):101-11. <https://doi.org/10.22270/jddtv12i4-S.5533>
19. Singh A, Raza A, Amin S, Damodaran C, Sharma AK. Recent Advances in the Chemistry and Therapeutic Evaluation of Naturally Occurring and Synthetic Withanolides. *Molecules.* 2022 Jan 28; 27(3):886. <https://doi.org/10.3390/molecules27030886>
20. Khan MA, Khan H, Khan S, Mahmood T, Khan PM, Jabar A. Anti-inflammatory, analgesic and antipyretic activities of *Physalis minima* Linn. *Journal of Enzyme Inhibition and Medicinal Chemistry.* 2009 Jun 1; 24(3):632-7. <https://doi.org/10.1080/14756360802321120>
21. Hung M, He JX, Hu HX, Zhang K, Wang XN, Zhao BB, Lou HX, Ren DM, Shen T. Withanolides from the genus *Physalis*: a review on their

phytochemical and pharmacological aspects. *Journal of Pharmacy and Pharmacology*. 2020 May; 72(5):649-69. <https://doi.org/10.1111/jphp.13209>

22. Shan-Shan WE, Cai-Yun GA, Rui-Jun LI, Ling-Yi KO, Jun LU. Withaniminimas A-F, six withanolides with potential anti-inflammatory activity from *Physalis minima*. *Chinese journal of natural medicines*. 2019 Jun 1; 17(6):469-74 [https://doi.org/10.1016/S1875-5364\(19\)30054-8](https://doi.org/10.1016/S1875-5364(19)30054-8)

23. Hauser AS, Attwood MM, Rask-Andersen M, Schiöth HB, Gloriam DE. Trends in GPCR drug discovery: new agents, targets and indications. *Nature reviews Drug discovery*. 2017; 16(12):829-42. <https://doi.org/10.1038/nrd.2017.178>

24. Daina A, Michielin O, Zoete V. SwissADME: a free web tool to evaluate pharmacokinetics, drug-likeness and medicinal chemistry friendliness of small molecules. *Scientific reports*. 2017; 7(1):1-3. <https://doi.org/10.1038/srep42717>

25. Guan L, Yang H, Cai Y, Sun L, Di P, Li W, Liu G, Tang Y. ADMET-score-a comprehensive scoring function for evaluation of chemical drug-likeness. *Medchemcomm*. 2019; 10(1):148-57. <https://doi.org/10.1039/C8MD00472B>

26. Bose PP, Chatterjee U, Hubatsch I, Artursson P, Govender T, Kruger HG, Bergh M, Johansson J, Arvidsson PI. In vitro ADMET and physicochemical investigations of poly-N-methylated peptides designed to inhibit A β aggregation. *Bioorganic & medicinal chemistry*. 2010; 18(16):5896-902. <https://doi.org/10.1016/j.bmc.2010.06.087>

27. Radchenko EV, Dyabina AS, Palyulin VA, Zefirov NS. Prediction of human intestinal absorption of drug compounds. *Russian Chemical Bulletin*. 2016; 65(2):576-80. <https://doi.org/10.1007/s11172-016-1340-0>

28. Alam A, Kowal J, Broude E, Roninson I, Locher KP. Structural insight into substrate and inhibitor discrimination by human P-glycoprotein. *Science*. 2019; 363(6428):753-6. <https://doi.org/10.1126/science.aav7102>

29. Daina A, Zoete V. A boiled-egg to predict gastrointestinal absorption and brain penetration of small molecules. *ChemMedChem*. 2016; 11(11):1117-21. <https://doi.org/10.1002/cmdc.201600182>

30. Liao M, Jaw-Tsai S, Beltman J, Simmons AD, Harding TC, Xiao JJ. Evaluation of in vitro absorption, distribution, metabolism, and excretion and assessment of drug-drug interaction of rucaparib, an orally potent poly (ADP-ribose) polymerase inhibitor. *Xenobiotica*. 2020; 50(9):1032-42. <https://doi.org/10.1080/00498254.2020.1737759>

31. Egan WJ, Merz KM, Baldwin JJ. Prediction of drug absorption using multivariate statistics. *Journal of medicinal chemistry*. 2000 Oct 19; 43(21):3867-77. <https://doi.org/10.1021/jm000292e>

32. Wessel MD, Jurs PC, Tolan JW, Muskal SM. Prediction of human intestinal absorption of drug compounds from molecular structure. *Journal of Chemical Information and Computer Sciences*. 1998 Jul 20; 38(4):726-35. <https://doi.org/10.1021/ci980029a>

33. Binkhathlan Z, Lavasanifar A. P-glycoprotein inhibition as a therapeutic approach for overcoming multidrug resistance in cancer: current status and future perspectives. *Current cancer drug targets*. 2013 Mar 1; 13(3):326-46. <https://doi.org/10.2174/15680096113139990076>

34. Naef, R. (2015). A generally applicable computer algorithm based on the group additivity method for the calculation of seven molecular descriptors: heat of combustion, logPO/W, logS, refractivity, polarizability, toxicity and logBB of organic compounds; scope and limits of applicability. *Molecules* 20:18279. <https://doi.org/10.3390/molecules201018279>

35. Elnaz Gozalpour, Rick Greupink, Heleen M. Wortelboer, Albert Bilos, Marieke Schreurs, Frans G. M. Russel, and Jan B. Koenderink . Interaction of Digitalis-Like Compounds with Liver Uptake Transporters NTCP, OATP1B1, and OATP1B3. *Molecular Pharmaceutics* 2014, 11 (6):1844-1855. <https://doi.org/10.1021/mp400699p>

36. Motohashi H, Inui KI. Organic cation transporter OCTs (SLC22) and MATEs (SLC47) in the human kidney. *The AAPS journal*. 2013 Apr; 15(2):581-8. <https://doi.org/10.1208/s12248-013-9465-7>

37. Ekins S, Crumb WJ, Sarazan RD, Wikle JH, Wrighton SA. Three-dimensional quantitative structure-activity relationship for inhibition of human ether-a-go-go-related gene potassium channel. *Journal of Pharmacology and Experimental Therapeutics*. 2002 May 1; 301(2):427-34. <https://doi.org/10.1124/jpet.301.2.427>

38. Schyman, P., R. Liu, and A. Wallqvist. General purpose 2D and 3D similarity approach to identify hERG blockers. *Journal of Chemical Information and Modeling*. 2016; 56(1):213-222. <https://doi.org/10.1021/acs.jcim.5b00616>

39. Schyman, P., R. Liu, V. Desai, and A. Wallqvist. vNN web server for ADMET predictions. *Frontiers in Pharmacology*. 2017 December 4; 8:889. <https://doi.org/10.3389/fphar.2017.00889>

40. Liu, R., G. Tawa, and A. Wallqvist. Locally weighted learning methods for predicting dose-dependent toxicity with application to the human maximum recommended daily dose. *Chemical Research in Toxicology*. 2012; 25(10):2216-2226. <https://doi.org/10.1021/tx300279f>

41. Liu, R., and A. Wallqvist. Merging applicability domains for in silico assessment of chemical mutagenicity. *Journal of Chemical Information and Modeling*. 2014; 54(3):793-800. <https://doi.org/10.1021/ci500016v>

42. Liu, R., P. Schyman, and A. Wallqvist. Critically assessing the predictive power of QSAR models for human liver microsomal stability. *Journal of Chemical Information and Modeling*. 2015; 55(8):1566-1575. <https://doi.org/10.1021/acs.jcim.5b00255>

43. Li, D., L. Chen, Y. Li, S. Tian, H. Sun, and T. Hou. ADMET evaluation in drug discovery. Development of in Silico prediction models for P-Glycoprotein substrates. 2014; 11(3):716-726. <https://doi.org/10.1021/mp400450m>

44. Broccatelli, F., E. Carosati, A. Neri, M. Frosini, L. Goracci, T. Oprea, and G. Cruciani. A novel approach for predicting P-Glycoprotein (ABCB1) inhibition using molecular interaction fields. 2011; 54(6):1740-1751. <https://doi.org/10.1021/jm101421d>

45. Chen, L., Y. Li, Q. Zhao, H. Peng, and T. Hou. ADME evaluation in drug discovery. Predictions of P-Glycoprotein inhibitors using recursive partitioning and naive Bayesian classification techniques. 2011; 8(3):889-900. <https://doi.org/10.1021/mp100465q>

46. Schyman, P., R. Liu, and A. Wallqvist. Using the variable-nearest neighbor method to identify P-glycoprotein substrates and inhibitors. *ACS Omega*. 2016; 1(5):923-929. <https://doi.org/10.1021/acsomega.6b00247>

47. Muehlbacher, M., G. Spitzer, K. Liedl, J. Kornhuber. Qualitative prediction of blood-brain barrier permeability on a large and refined dataset. *Journal of Computer-Aided Molecular Design*. 2011; 25:1095. <https://doi.org/10.1007/s10822-011-9478-1>

48. Xu, Y., Z. Dai, F. Chen, S. Gao, J. Pei, and L. Lai. Deep learning for drug-induced liver injury. 2015, 55 (10):2085-2093. <https://doi.org/10.1021/acs.jcim.5b00238>

49. Attene-Ramos, M., R. Huang, S. Michael, K. Witt, A. Richard, R. Tice, A. Simeonov, C. Austin, M. Xia. Profiling of the Tox21 chemical collection for mitochondrial function to identify compounds that acutely decrease mitochondrial membrane potential. 2015; 123(1):49. <https://doi.org/10.1289/ehp.1408642>

50. Choi JM, Oh SJ, Lee JY, Jeon JS, Ryu CS, Kim YM, Lee K, Kim SK. Prediction of drug-induced liver injury in HepG2 cells cultured with human liver microsomes. *Chemical Research in Toxicology*. 2015 18; 28(5):872-85. <https://doi.org/10.1021/tx500504n>

51. Pelkonen O, Turpeinen M, Hakkola J, Honkakoski P, Hukkanen J, Raunio H. Inhibition and induction of human cytochrome P450 enzymes: current status. *Archives of toxicology*. 2008 Oct; 82(10):667-715. <https://doi.org/10.1007/s00204-008-0332-8>

52. Ramya S, Neethirajan K, Jayakumararaj R. Profile of bioactive compounds in *Syzygium cumini*-a review. *J. Pharm. Res.* 2012 Aug;5(8):4548-53.

53. Loganathan T, Barathinivas A, Soorya C, Balamurugan S, Nagajothi TG, Jayakumararaj R. GCMS Profile of Bioactive Secondary Metabolites with Therapeutic Potential in the Ethanolic Leaf Extracts of *Azadirachta indica*: A Sacred Traditional Medicinal Plant of INDIA. *Journal of Drug Delivery and Therapeutics*. 2021 Aug 15; 11(4-S):119-26. <https://doi.org/10.22270/jddt.v11i4-S.4967>

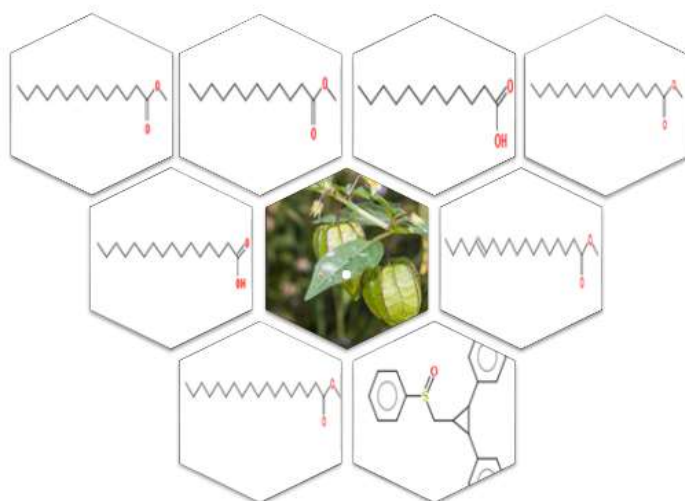


Figure 1: Range of Bioactive Compounds in PMELE

Table 1a: GCMS analysis of Bioactive Compounds in PMELE

S.No	RT (min)	COMPOUND	MF	MW	PA (%)
1.	23.757	Dodecanoic acid, methyl ester	C ₁₃ H ₂₆ O ₂	214.34	21.85
2.	26.148	Dodecanoic acid	C ₁₂ H ₂₄ O ₂	200.32	9.06
3.	28.392	Methyl tetradecanoate	C ₁₅ H ₃₀ O ₂	242.40	11.43
4.	32.479	Hexadecanoic acid, methyl ester	C ₁₇ H ₃₄ O ₂	270.50	7.85
5.	34.028	n-Hexadecanoic acid	C ₁₆ H ₃₂ O ₂	256.42	4.47
6.	35.812	trans-13-Octadecenoic acid, methyl ester	C ₁₉ H ₃₆ O ₂	296.50	7.45
7.	36.27	Methyl stearate	C ₁₉ H ₃₈ O ₂	298.50	3.11
8.	41.908	(2,3-Diphenylcyclopropyl) methyl phenyl sulfoxide, Z,	C ₂₂ H ₂₀ OS	332.50	10.64

Table 1b: IUPAC, CID and SMILES of Bioactive Compounds in PMELE

IUPAC Name of Compound	CID	Canonical SMILES
Dodecanoic acid, methyl ester	8139	CCCCCCCCCC(=O)OC
Dodecanoic acid	3893	CCCCCCCCCC(=O)O
Methyl tetradecanoate	31284	CCCCCCCCCCCC(=O)OC
Hexadecanoic acid, methyl ester	8181	CCCCCCCCCCCCCCCC(=O)OC
n-Hexadecanoic acid	985	CCCCCCCCCCCCCCCC(=O)O
trans-13-Octadecenoic acid, methyl ester	5364506	CCCC/C=C/CCCCCCCCCCCC(=O)OC
Methyl stearate	8201	CCCCCCCCCCCCCCCC(=O)OC
(2,3-Diphenylcyclopropyl) methyl phenyl sulfoxide, Z,	562543	C1=CC=C(C=C1)C2C(C2C3=CC=CC=C3)CS(=O)C4=CC=CC=C4

Table 2a: Biomolecular properties attributes of Methyl dodecanoate

originalSMILES CCCCCCCCC(=O)OC miSMILES: CCCCCCCCC(=O)OC	Molecular Properties		Calculated Values	
	miLogP		5.35	
	TPSA		26.30	
	Natoms		15	
	MW		214.35	
	nON		2	
	nOHNH		0	
	Nviolations		1	
	Nrotb		11	
	volume		214.74	
Biological Properties		Bioactivity Scores		
GPCR ligand		-0.41		
Ion channel modulator		-0.13		
Kinase inhibitor		-0.73		
Nuclear receptor ligand		-0.43		
Protease inhibitor		-0.46		
Enzyme inhibitor		-0.11		

Table 2b: Biomolecular properties attributes of Lauric acid

		Molecular Properties	Calculated Values
originalSMILES	CCCCCCCCCCCC(=O)O	miLogP	5.04
miSMILES:	CCCCCCCCCCCC(=O)O	TPSA	37.30
		Natoms	14
		MW	200.32
		nON	2
		nOHNH	1
		Nviolations	1
		Nrotb	10
		volume	224.22
		Biological Properties	Bioactivity Scores
		GPCR ligand	-0.27
		Ion channel modulator	-0.04
		Kinase inhibitor	-0.75
		Nuclear receptor ligand	-0.24
		Protease inhibitor	-0.36
		Enzyme inhibitor	0.04

Table 2c: Biomolecular properties attributes of Methyl tetradecanoate

		Molecular Properties	Calculated Values
originalSMILES	CCCCCCCCCCCCCCC(=O)OC	miLogP	6.36
miSMILES:	CCCCCCCCCCCCCCC(=O)OC	TPSA	26.30
		Natoms	17
		MW	242.40
		nON	2
		nOHNH	0
		Nviolations	1
		Nrotb	13
		volume	275.35
		Biological Properties	Bioactivity Scores
		GPCR ligand	-0.24
		Ion channel modulator	-0.07
		Kinase inhibitor	-0.51
		Nuclear receptor ligand	-0.24
		Protease inhibitor	-0.28
		Enzyme inhibitor	-0.02

Table 2d: Biomolecular properties attributes of trans-13-Octadecenoic acid, methyl ester

		Molecular Properties	Calculated Values
originalSMILES	CCCCCCCCCCCCCCC(=O)OC	miLogP	7.37
miSMILES:	CCCCCCCCCCCCCCC(=O)OC	TPSA	26.30
	Methyl palmitate	Natoms	19
		MW	270.46
		nON	2
		nOHNH	0
		Nviolations	1
		Nrotb	15
		volume	308.95
		Biological Properties	Bioactivity Scores
		GPCR ligand	-0.11
		Ion channel modulator	-0.05
		Kinase inhibitor	-0.34
		Nuclear receptor ligand	-0.09
		Protease inhibitor	-0.13
		Enzyme inhibitor	-0.04

Table 2e: Biomolecular properties attributes of Palmitic acid

		Molecular Properties	Calculated Values
originalSMILES	CCCCCCCCCCCCCCCC(=O)O	miLogP	7.06
miSMILES:	CCCCCCCCCCCCCCCC(=O)O	TPSA	37.30
		Natoms	18
		MW	256.43
		nON	2
		nOHNH	1
		Nviolations	1
		Nrotb	14
		volume	291.42
		Biological Properties	Bioactivity Scores
		GPCR ligand	0.02
		Ion channel modulator	0.06
		Kinase inhibitor	-0.33
		Nuclear receptor ligand	0.08
		Protease inhibitor	-0.04
		Enzyme inhibitor	0.18

Table 2f: Biomolecular properties attributes of trans-13-Octadecenoic acid, methyl ester

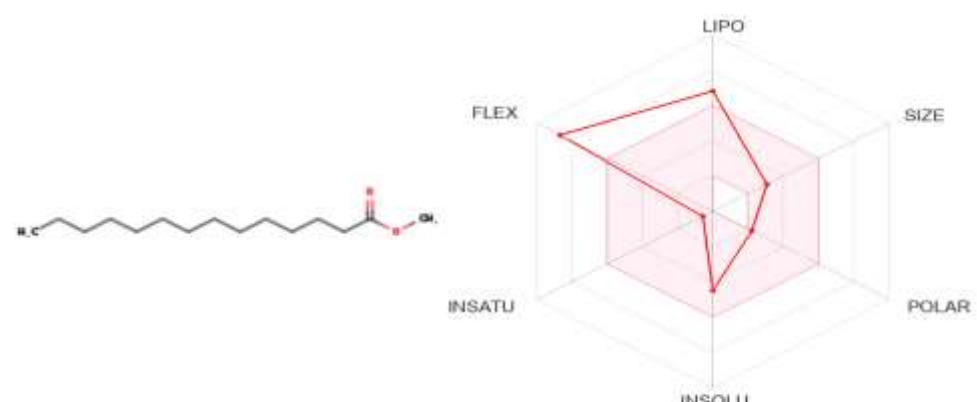
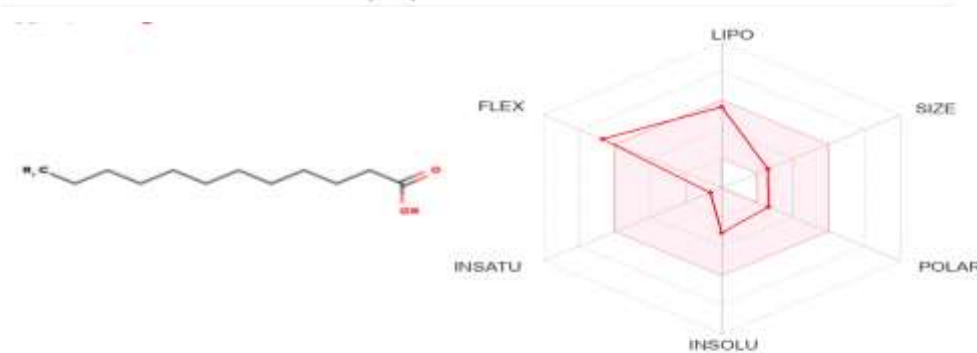
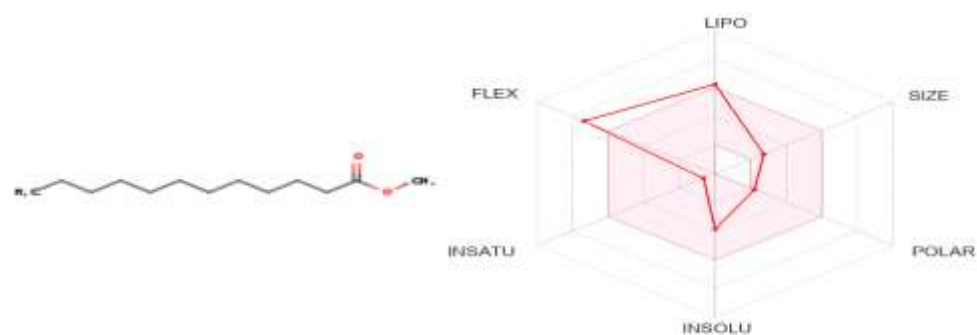
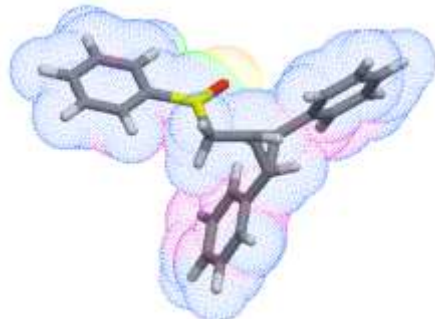
		Molecular Properties	Calculated Values
originalSMILES	CCCC/C=C/CCCCCCCCCCCC(=O)OC	miLogP	7.89
miSMILES:	CCCC/C=C/CCCCCCCCCCCC(=O)OC	TPSA	26.30
		Natoms	21
		MW	296.50
		nON	2
		nOHNH	0
		Nviolations	1
		Nrotb	16
		volume	336.37
		Biological Properties	Bioactivity Scores
		GPCR ligand	0.03
		Ion channel modulator	-0.03
		Kinase inhibitor	-0.25
		Nuclear receptor ligand	0.06
		Protease inhibitor	-0.02
		Enzyme inhibitor	0.12

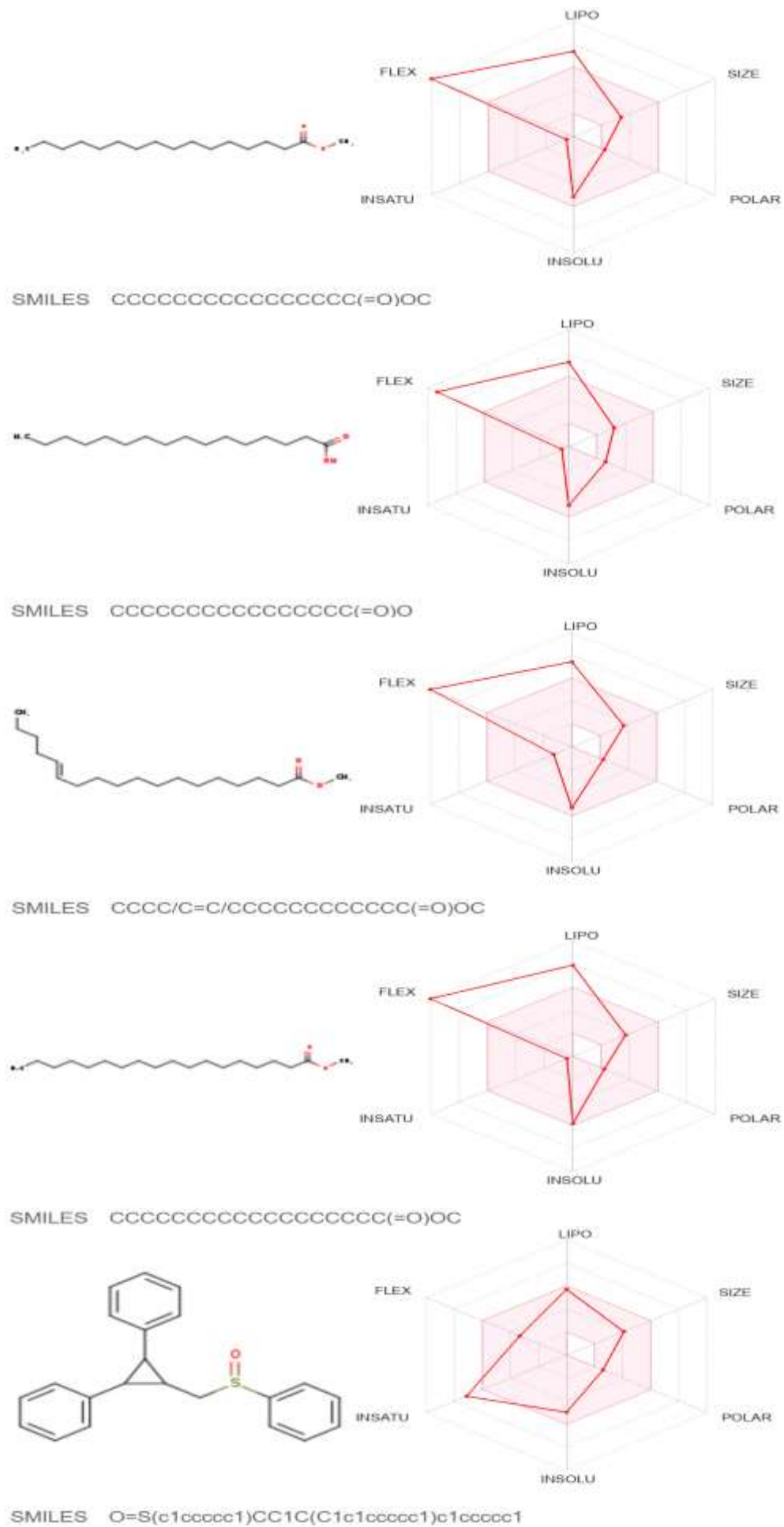
Table 2g: Biomolecular properties attributes of Methyl stearate

		Molecular Properties	Calculated Values
originalSMILES	CCCCCCCCCCCCCCCC(=O)OC	miLogP	8.32
miSMILES:	CCCCCCCCCCCCCCCC(=O)OC	TPSA	26.30
		Natoms	21
		MW	298.51
		nON	2
		nOHNH	0
		Nviolations	1
		Nrotb	17
		volume	342.55
		Biological Properties	Bioactivity Scores
		GPCR ligand	-0.03
		Ion channel modulator	-0.04
		Kinase inhibitor	-0.23
		Nuclear receptor ligand	0.00
		Protease inhibitor	-0.03
		Enzyme inhibitor	0.05

Table 2h: Biomolecular properties attributes of (2,3 Diphenylcyclopropyl)methyl phenyl sulfoxide

originalSMILES	Molecular Properties		Calculated Values	
C1=CC=C(C=C1)C2C(C2C3=CC=CC=C3)CS(=O)C4=CC=C C=C4 miSMILES: C1=CC=C(C=C1)C2C(C2C3=CC=CC=C3)CS(=O)C4=CC=C C=C4	miLogP		4.32	
	TPSA		17.07	
	Natoms		24	
	MW		332.47	
	nON		1	
	nOHNH		0	
	Nviolations		0	
	Nrotb		5	
	volume		308.98	
Biological Properties		Bioactivity Scores		
	GPCR ligand		0.15	
	Ion channel modulator		0.08	
	Kinase inhibitor		0.10	
	Nuclear receptor ligand		0.01	
	Protease inhibitor		0.27	
	Enzyme inhibitor		0.20	



Figure 2: Swiss ADME bioavailability radar reports for *P. minima* PBNPs

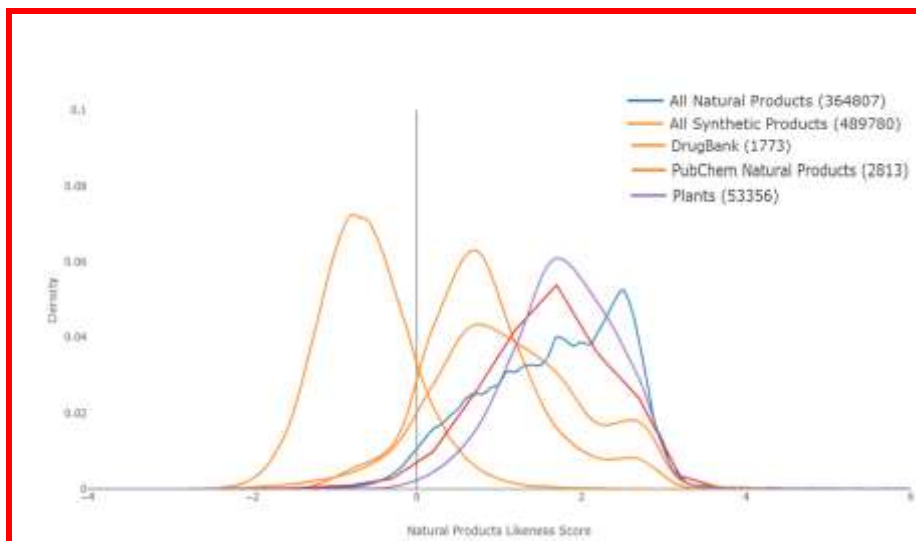
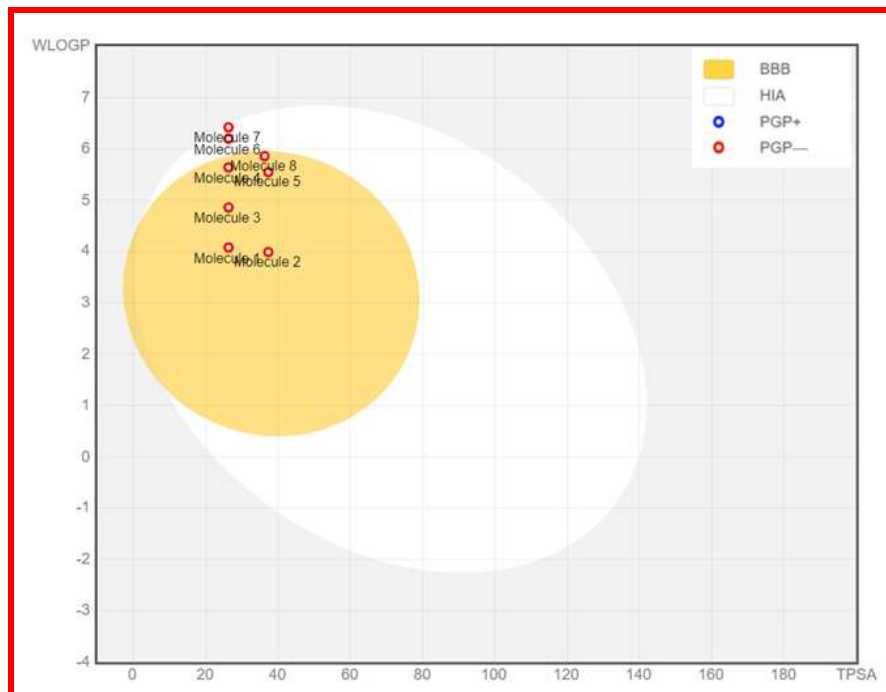
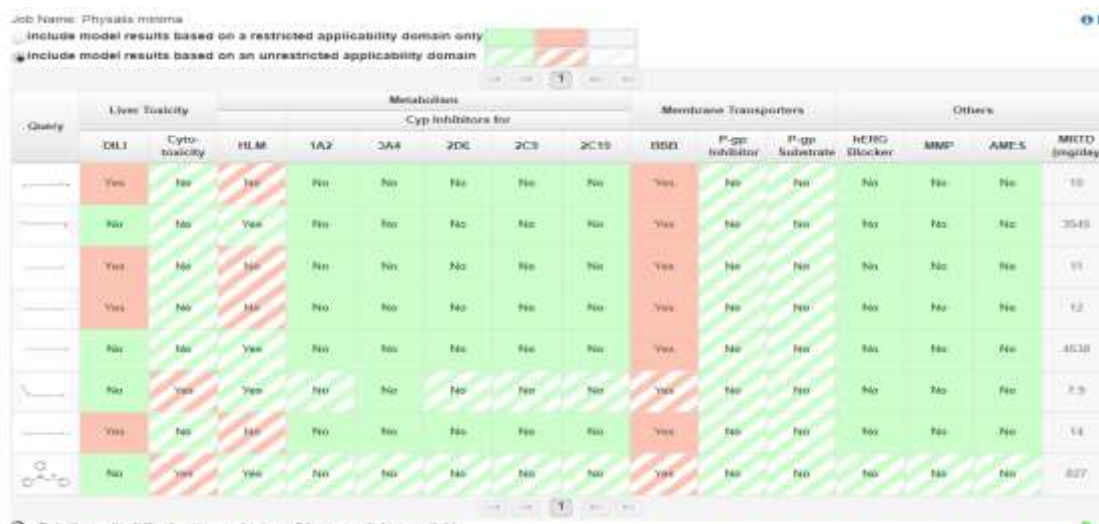
Figure 3: NaPLeS - Natural Product Likeness Score for PBNNPs from *P. minima*Figure 4: BOILED-Egg model for bioactive compounds from *P. minima*

Figure 5: Performance measures of vNN models for PBNNPs from PMELE

Table 3: Performance measures of vNN models in 10-fold cross validation using a restricted or unrestricted applicability domain for PBNPs from PMELE

Model	Data ^a	d ₀ ^b	h ^c	Accuracy	Sensitivity	Specificity	kappa	R ^d	Coverage
DILI	1427	0.60	0.50	0.71	0.70	0.73	0.42		0.66
		1.00	0.20	0.67	0.62	0.72	0.34		1.00
Cytotox (hep2g)	6097	0.40	0.20	0.84	0.88	0.76	0.64		0.89
		1.00	0.20	0.84	0.73	0.89	0.62		1.00
HLM	3219	0.40	0.20	0.81	0.72	0.87	0.59		0.91
		1.00	0.20	0.81	0.70	0.87	0.57		1.00
CYP1A2	7558	0.50	0.20	0.90	0.70	0.95	0.66		0.75
		1.00	0.20	0.89	0.61	0.95	0.60		1.00
CYP2C9	8072	0.50	0.20	0.91	0.55	0.96	0.54		0.76
		1.00	0.20	0.90	0.44	0.96	0.46		1.00
CYP2C19	8155	0.55	0.20	0.87	0.64	0.93	0.58		0.76
		1.00	0.20	0.86	0.52	0.94	0.50		1.00
CYP2D6	7805	0.50	0.20	0.89	0.61	0.94	0.57		0.75
		1.00	0.20	0.88	0.52	0.95	0.51		1.00
CYP3A4	10373	0.50	0.20	0.88	0.76	0.92	0.68		0.78
		1.00	0.20	0.88	0.69	0.93	0.64		1.00
BBB	353	0.60	0.20	0.90	0.94	0.86	0.80		0.61
		1.00	0.10	0.82	0.88	0.75	0.64		1.00
Pgp Substrate	822	0.60	0.20	0.79	0.80	0.79	0.58		0.66
		1.00	0.20	0.73	0.73	0.74	0.47		1.00
Pgp Inhibitor	2304	0.50	0.20	0.85	0.91	0.73	0.66		0.76
		1.00	0.10	0.81	0.86	0.74	0.61		1.00
hERG	685	0.70	0.70	0.84	0.84	0.83	0.68		0.80
		1.00	0.20	0.82	0.82	0.83	0.64		1.00
MMP	6261	0.50	0.40	0.89	0.64	0.94	0.61		0.69
		1.00	0.20	0.87	0.52	0.94	0.50		1.00
AMES	6512	0.50	0.40	0.82	0.86	0.75	0.62		0.79
		1.00	0.20	0.79	0.82	0.75	0.57		1.00
MRTD ^e	1184	0.60	0.20					0.79	0.69
		1.00	0.20					0.74	1.00

^aNumber of compounds in the dataset; ^bTanimoto-distance threshold value; ^cSmoothing factor; ^dPearson's correlation coefficient ; ^eRegression model

Table 4: Summary of ADMET properties of PBNPs (C1-C8) from PMELE

PROPERTY	MODEL NAME	C1	C2	C3	C4	C5	C6	C7	C8
Absorption	Water solubility	-5.096	-4.181	-6.109	-6.927	-5.562	-7.436	-7.51	-6.343
Absorption	Caco2 permeability	1.604	1.562	1.602	1.6	1.558	1.605	1.598	1.358
Absorption	Intestinal absorption (human)	93.709	93.379	93.022	92.335	92.004	92.154	91.648	96.826
Absorption	Skin Permeability	-1.844	-2.693	-2.244	-2.595	-2.717	-2.758	-2.792	-2.698
Absorption	P-glycoprotein substrate	No	No	No	No	No	No	Yes	
Absorption	P-glycoprotein I inhibitor	No	No	No	No	No	No	Yes	
Absorption	P-glycoprotein II inhibitor	No	No	No	No	No	Yes	Yes	Yes
Distribution	VDss (human)	0.256	-0.631	0.311	0.334	-0.543	0.299	0.325	0.264
Distribution	Fraction unbound (human)	0.23	0.26	0.142	0.074	0.101	0.027	0.027	0.04
Distribution	BBB permeability	0.674	0.057	0.711	0.749	-0.111	0.777	0.787	0.898
Distribution	CNS permeability	-1.897	-2.034	-1.788	-1.678	-1.816	-1.516	-1.569	-1.039
Metabolism	CYP2D6 substrate	No							
Metabolism	CYP3A4 substrate	No	No	Yes	Yes	Yes	Yes	Yes	Yes
Metabolism	CYP1A2 inhibitiior	No	No	Yes	Yes	No	Yes	Yes	Yes
Metabolism	CYP2C19 inhibitiior	No	Yes						
Metabolism	CYP2C9 inhibitiior	No	Yes						
Metabolism	CYP2D6 inhibitiior	No							
Metabolism	CYP3A4 inhibitiior	No							
Excretion	Total Clearance	1.724	1.623	1.793	1.861	1.763	1.978	1.929	0.24
Excretion	Renal OCT2 substrate	No							
Toxicity	AMES toxicity	No	Yes						
Toxicity	Max. tolerated dose (human)	0.351	-0.34	0.257	0.178	-0.708	0.04	0.099	0.454
Toxicity	hERG I inhibitor	No							
Toxicity	hERG II inhibitor	No	Yes						
Toxicity	Oral Rat Acute Toxicity (LD50)	1.661	1.511	1.636	1.635	1.44	1.637	1.656	3.143
Toxicity	Oral Rat Chronic Toxicity (LOAEL)	2.707	2.89	2.851	2.998	3.181	3.075	3.147	0.488
Toxicity	Hepatotoxicity	No	Yes						
Toxicity	Skin Sensitisation	Yes	No						
Toxicity	T.Pyriformis toxicity	2.047	0.954	2.208	1.935	0.84	1.529	1.448	0.38
Toxicity	Minnow toxicity	-0.374	-0.084	-0.891	-1.373	-1.083	-1.727	-1.854	-0.561